MHD POISEUILLE FLOW WITH SORET AND DUFOUR EFFECTS UNDER SLIP BOUNDARY CONDITIONS

U. J. DAS

Department of Mathematics, Gauhati University, Guwahati-781014, Assam, India.
Email: utpaljyotidas@yahoo.co.in

***Abstract*— A steady MHD flow is analyzed in presence of Soret and Dufour effects with consideration of induced magnetic field under slip boundary conditions. The walls of the channel are porous, isothermal and subjected to injection/suction at a constant velocity. The effects of various flow parameters on velocity, magnetic field intensity, temperature, concentration, skin friction, Nusselt number and Sherwood number are discussed.**

***Keywords*— MHD, Poiseuille flow, Navier Slip, thermal radiation, induced magnetic field.**

I. INTRODUCTION

The prediction of MHD channel flows with heat and mass transfer is encountered in many engineering and scientific applications. MHD channel flows are studied by various authors Soundalgekar and Bhatt (1984), Cox (1991), Makinde and Mhone (2005), Choudhury and Das (2012), Das (2017), Srinivas *et al.* (2018). The effects of Soret and Dufour can play an important role in many practical applications of areas such as chemical engineering and geosciences. In this line many authors Alam and Rahman (2006), Makinde (2011), Turkyilmazoglu and Pop (2012), Bilal *et al.* (2015), Hayat *et al.* (2018) have studied. The no-slip condition at the boundary surface is not valid in some physical situations. In this regard many authors Beavers and Joseph (1967), Khaled and Vafai (2004), Makinde and Osalusi (2006), Soltani and Yilmazer (1998), Adesanya and Makinde (2014), Mehmood and Ali (2007), Misra and Adhikary (2016) reported several important phenomena. Ahmed (2019) recently carried out an analysis of heat and mass transfer on steady MHD Poiseuille flow in presence of induced magnetic field and Soret effect. Recently, Divya *et al.* (2019), Manjunatha *et al.* (2019, 2020) have studied the peristaltic flow of Jeffery fluid in channel with slip effects.

The objective of the proposed work is to extend the study of Ahmed (2019) incorporating the thermal radiation and Dufour effect under slip boundary conditions. The effect of slip is assumed to be Navier slip which depends on shear stress at both the permeable walls as applied by Mehmood and Ali (2007).

II. MATHEMATICAL FORMULATION

Consider a steady laminar flow of an electrically conducting, viscous, incompressible fluid between two permeable, isothermal, stationary walls. The walls are separated at a distance $2a$ and subjected to a constant suction/ injection velocity. The $\bar{x}$- axis is taken along the centre of the channel, $\bar{y}$-axis perpendicular to it, and $\bar{z}$-axis along the width of the walls (Fig. 1). Magnetic field of uniform strength H_0 is imposed normal to the channel wall so that it produces an induced magnetic field $H = (H_{\bar{x}}, H_{\bar{y}}, 0)$ at a point $(\bar{x}, \bar{y}, \bar{z})$. Navier boundary slip condition assumes that the velocity, $\bar{u}$, at the solid wall is proportional to the shear stress at the solid wall i.e. $\bar{u} = \bar{\lambda}\frac{\partial \bar{u}}{\partial \bar{y}}$ where $\bar{\lambda}$ is slip parameter. Assuming the width of the walls is very large in comparison to the distance between the walls, the flow becomes two dimensional and the governing equations of the flow become (Ahmed, 2019):

$$\frac{\partial \bar{v}}{\partial \bar{y}} = 0 \Rightarrow \bar{v} = -V, \text{ (a constant)} \tag{1}$$

$$\frac{\partial H_{\bar{y}}}{\partial \bar{y}} = 0 \Rightarrow H_{\bar{y}} = H_0, \text{ (a constant)} \tag{2}$$

$$\rho\left(\upsilon\frac{\partial^2 \bar{u}}{\partial \bar{y}^2} + V\frac{\partial \bar{u}}{\partial \bar{y}}\right) + \mu_e H_0 \frac{\partial H_{\bar{x}}}{\partial \bar{y}} = \frac{\partial P'}{\partial \bar{y}} = -\bar{P}, \tag{3}$$

$$\eta\frac{\partial^2 H_{\bar{x}}}{\partial \bar{y}^2} + V\frac{\partial H_{\bar{x}}}{\partial \bar{y}} + H_0\frac{\partial \bar{u}}{\partial \bar{y}} = 0, \tag{4}$$

$$-\rho C_p V\frac{\partial T}{\partial \bar{y}} = \kappa\frac{\partial^2 T}{\partial \bar{y}^2} + \frac{1}{\sigma}\left(\frac{\partial H_{\bar{x}}}{\partial \bar{y}}\right)^2 - \frac{\partial q_r}{\partial \bar{y}} + \mu\left(\frac{\partial \bar{u}}{\partial \bar{y}}\right)^2 + \frac{\rho D_m K_T}{C_s}\frac{\partial^2 C}{\partial \bar{y}^2}, \tag{5}$$

$$-V\frac{\partial C}{\partial \bar{y}} = D_m\frac{\partial^2 C}{\partial \bar{y}^2} + \frac{D_m K_T}{T_m}\frac{\partial^2 T}{\partial \bar{y}^2}, \tag{6}$$

with boundary conditions (Mehmood and Ali, 2007; Ahmed, 2019)

$$\bar{u} = \bar{\lambda}\frac{\partial \bar{u}}{\partial \bar{y}}, T = T_s, C = C_s, H_{\bar{x}} = 0 \text{ at } \bar{y} = -a, \tag{7}$$

$$\bar{u} = \bar{\lambda}\frac{\partial \bar{u}}{\partial \bar{y}}, T = T_s, C = C_s, H_{\bar{x}} = 0 \text{ at } \bar{y} = a.$$

Introduce the following non-dimensional parameters

$$y = \frac{\bar{y}}{L}, u = \frac{\bar{u}}{V}, \theta = \frac{T - T_0}{T_s}, \phi = \frac{C - C_0}{C_s} \tag{8}$$

$$\mathrm{Re} = \frac{VL}{\upsilon}, Rm = \frac{VL}{\eta}, H_x = \frac{H_{\bar{x}}}{H_0}, \Pr = \frac{\mu C_p}{\kappa}, M^2 = \frac{\mu_e H_0^2 L}{V\mu},$$

$$P = \frac{\bar{P}L}{\rho V^2}, Sc = \frac{\upsilon}{D_m}, Ec = \frac{V^2}{C_p T_s}, Sr = \frac{D_m K_T T_s}{\upsilon C_s T_m}, Du = \frac{D_m K_T}{\upsilon C_p T_s},$$

$$N = \frac{4\bar{\sigma}T_s^3}{\kappa\bar{\alpha}}, \lambda = \frac{\bar{\lambda}}{L}.$$

The Rosseland approximation (Brewster, 1992) is

$$q_r = -\frac{4\bar{\sigma}}{3\bar{\alpha}}\frac{\partial T^4}{\partial \bar{y}} + \frac{D_m K_T}{T_m}\frac{\partial^2 T}{\partial \bar{y}^2}, \tag{9}$$

Assuming T^4 as a linear function of temperature, we get

$$T^4 = 4T_s^3 T - 3T_s^4. \tag{10}$$

Using (8)-(10), the non-dimensional form of equations (3) - (6) become

$$\frac{d^2 u}{dy^2} + \mathrm{Re}\frac{du}{dy} + M^2\frac{dH_{\bar{x}}}{dy} = -P\mathrm{Re}, \tag{11}$$

$$\frac{d^2 H_x}{dy^2} + Rm\frac{dH_x}{dy} + Rm\frac{du}{d\bar{y}} = 0, \tag{12}$$

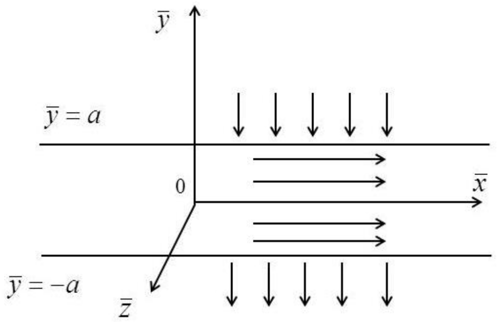

Figure1: Flow configuration.

$$Rm\left(1+\frac{4N}{3}\right)\frac{d^2\theta}{dy^2}+\mathrm{Re}Rm\mathrm{Pr}\frac{d\theta}{dy}+Rm\mathrm{Pr}Ec\left(\frac{du}{dy}\right)^2 \quad (13)$$
$$+\mathrm{Pr}EcM^2\left(\frac{dH_x}{dy}\right)^2+RmDu\mathrm{Pr}\frac{d^2\phi}{dy^2}=0,$$
$$\frac{d^2\phi}{dy^2}+Sc\mathrm{Re}\frac{d\phi}{dy}+ScSr\frac{d^2\theta}{dy^2} \quad (14)$$

with boundary conditions

$$u=\left[\lambda\frac{du}{dy}\right]_{y=\pm1}, \theta=0, \phi=0, H_x=0 \text{ at } y=\pm1 \quad (15)$$

where Re, M, P, Rm, N, Pr, Ec, Du, Sc, λ are Reynolds number, Hartmann number, non-dimensional pressure gradient, magnetic Prandtl number, radiation parameter, Prandtl number, Eckert number, Soret number, Dufour number, Schmidt number, and slip parameter respectively.

The skin friction at the lower wall is obtained as $\tau=\left[\frac{du}{dy}\right]_{y=-1}$.

The Nusselt number at the lower wall is $Nu=-\left[\frac{d\theta}{dy}\right]_{y=-1}$.

The Sherwood number at the lower wall is $Sh=-\left[\frac{d\phi}{dy}\right]_{y=-1}$.

III. RESULTS AND DISCUSSION

The governing Eqs. (11)-(14) under boundary condition (15) are solved numerically using MATLAB bvp4c method.

It is to be worth to mention here that by setting $\lambda=0$, $N=0$, $Du=0$ the present work coincided with the work of Ahmed (2019).

Here, numerical computations are carried out with the values of the physical parameters at $R\mathrm{m}=2$, $M=3$, $P=10$, $\mathrm{R}e=1$, $\mathrm{P}r=0.71$, $N=1$, $Du=0.5$, $Sr=0.5$, $Sc=0.62$, $Ec=0.6$, $\lambda=0.2$.

Figures 2-5 shows the fluid velocity u for different values of slip parameter λ, magnetic Reynolds number Rm, pressure gradient P with $\lambda=0$ and $\lambda=0.2$, respectively. Figure 2 reveal that the slip effects reduces the fluid velocity in the channel except adjacent to the lower wall of the channel where opposite effect is seen for $y<-0.4$. Figure 3 shows that the fluid velocity decreases in the central part of the channel as Rm increases, but reverse effect is seen near the walls of the channel in the region $y<-0.8$ or $y>0.8$. Figures 4 and 5 shows that the fluid velocity increases in the central part of the channel irrespective of the slip parameter with the increasing values of the pressure gradient, whereas fluid velocity decreases near the upper wall (Fig. 5) for $y>0.8$ due to the

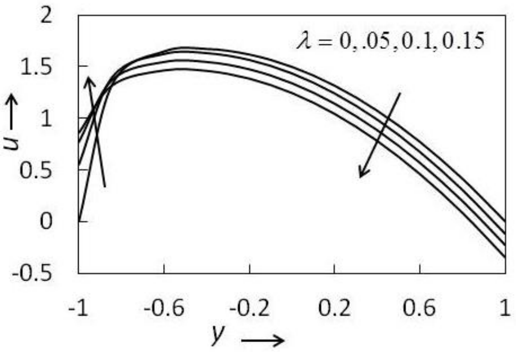

Figure 2: variation of u for various λ.

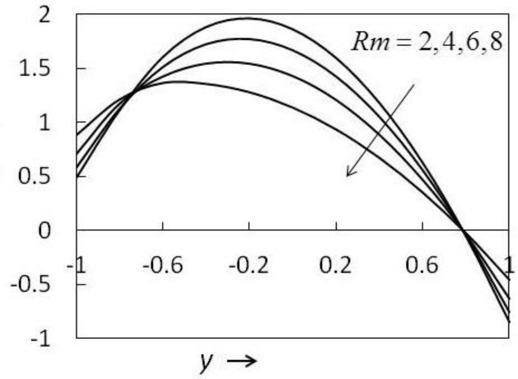

Figure 3: Variation of u for various Rm.

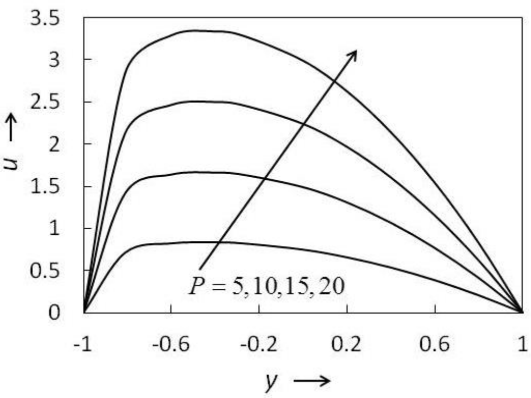

Figure 4: Variation of u for various P with $\lambda=0$.

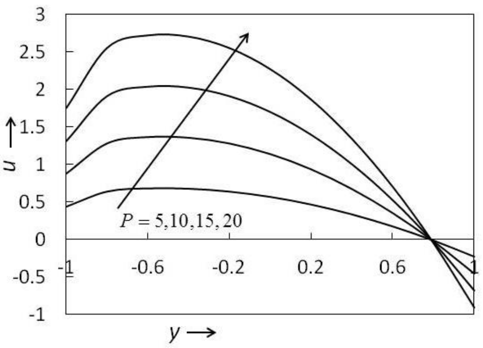

Figure 5: Variation of u for various P with $\lambda=0.2$.

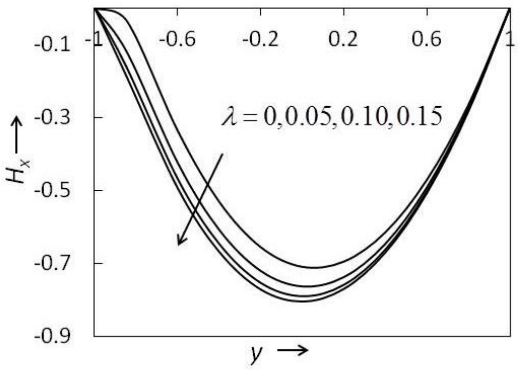

Figure 6: Variation of H_x for various λ.

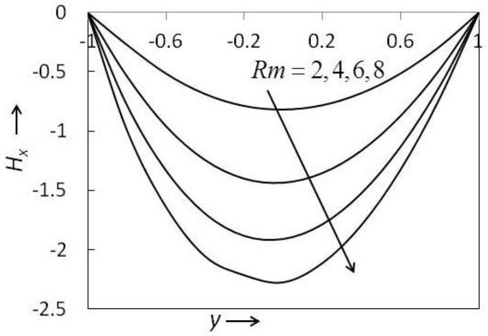

Figure 7: Variation of H_x for various Rm.

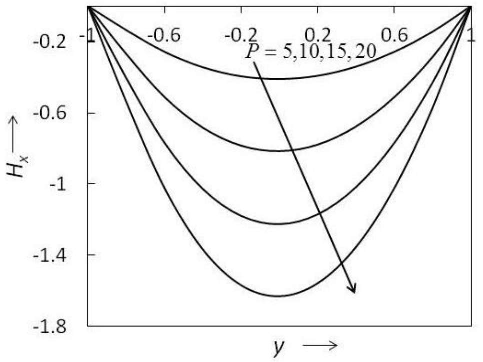

Figure 8: Variation of H_x for various P with $\lambda = 0.2$.

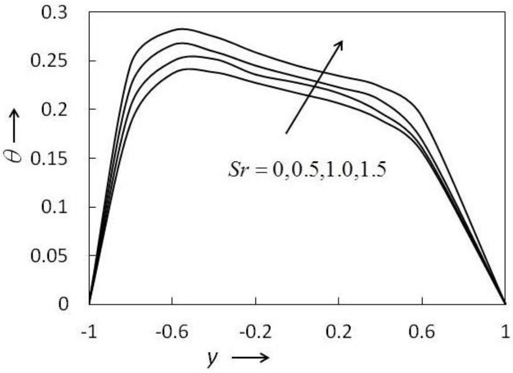

Figure 9: Variation of θ for various Sr.

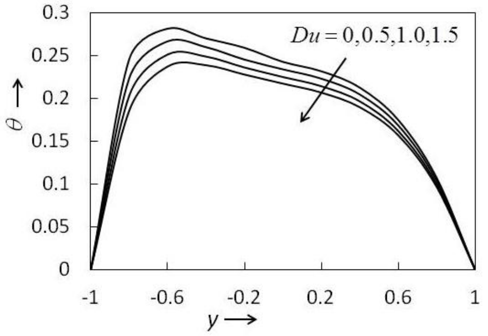

Figure 10: Variation of θ for various Du.

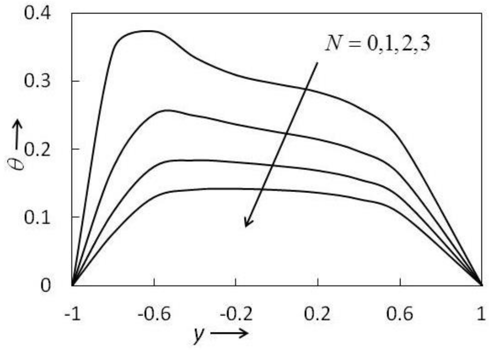

Figure 11: Variation of θ for various N.

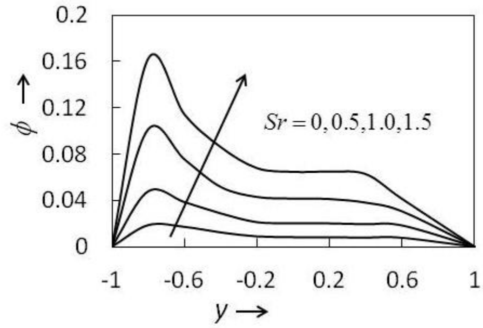

Figure 12: Variation of ϕ for various Sr.

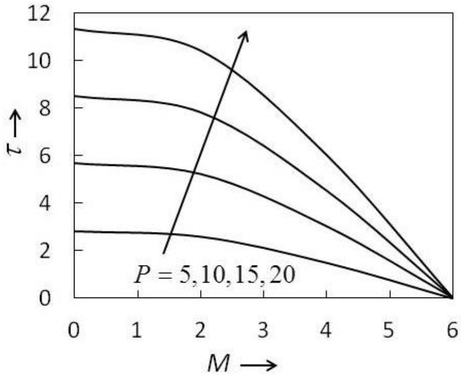

Figure 13: Variation of τ at lower wall for various P.

presence of slip parameter with the increasing values of pressure gradient.

Figures 6-8 represents the distribution of the induced magnetic field intensity H_x at various values of slip parameter, magnetic Reynolds number, and pressure gradient respectively. It is seen that H_x reduced with the increase in slip parameter (Fig. 6) from $\lambda = 0$ to $\lambda = 0.15$ through 0.5, 1.0 and magnetic Reynolds number from $Rm = 2$ to $Rm = 8$ through 4 and 6 Also, Fig. 8 shows that H_x reduces due an increase in P from P=5 to P=20 through 10, 15.

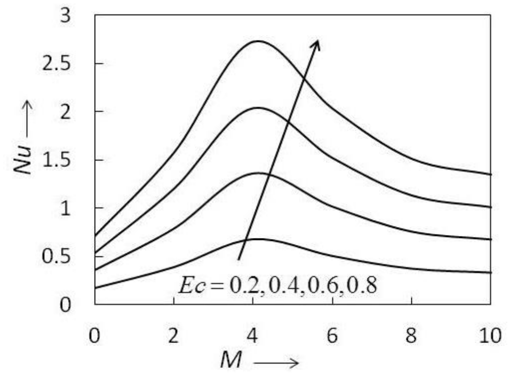

Figure 14: Variation of Nu at lower wall for various Ec.

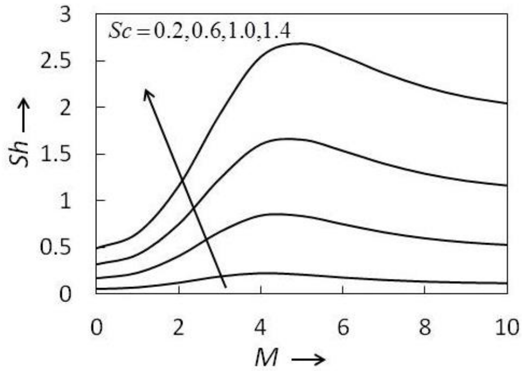

Figure 15: Variation of Sh at lower wall for various Sc.

Figures 9-11 reveal that at any given distance the temperature increases as the Soret number increases (Fig. 9), whereas it reduces with the increase in Dufour number (Fig. 10) and thermal radiation parameter (Fig. 11). The concentration distribution for various values of Sr is shown in Fig. 12. It is observed that there is a significant rise in the fluid concentration due to the increase in Sr and this rise is more prominent near the lower wall when Sr<-0.7.

Figure 13 shows the skin friction coefficient τ at the lower wall against Hartmann number for various P. It is seen that τ at the lower wall decrease with an increase in M. Also, it reveal that τ increase with increasing pressure gradient.

It is shown in Fig.14 that Nusselt number Nu increases at the lower wall with the increase in Eckert number Ec from Ec=0.2 to Ec=0.8 through 0.4 and 0.6. Also, it is seen that Nu rises when $M < 4$ and it decreases gradually when $M > 4$.

Figure 15 shows that Sherwood number Sh rises with the increase in Schmidt number from $Sc = 0.2$ to $Sc = 1.4$ through 1.0 and 1.4. Also, the rate of mass transfer Sh rises for $M < 4.5$ and it decreases gradually when $M > 4.5$.

IV. CONCLUSIONS

The effects of slip on a steady MHD Poiseuille flow with Soret and Dufour effects have been studied. The main conclusions are

1. Slip velocity and magnetic Reynolds number reduces the fluid velocity in the central part of the channel. Also, slip parameter and magnetic Reynolds number reduces the magnetic field intensity in the channel.
2. Fluid velocity increases due to the growth in pressure gradient, but magnetic field intensity in the channel decreases.
3. Fluid temperature reduces due to the increase in Dufour number and thermal radiation parameter.
4. Fluid Temperature and concentration increases as the Soret number increases.
5. Skin friction at the lower wall increase with the increase in pressure gradient, whereas it decreases with an increase in Hartmann number.
6. Nusselt number at the lower wall increases with an increase in Eckert nmber.
7. Sherwood number at the lower wall increase with an increase in Schmidt number.

NOMENCLATURE

a: half of the distance between the walls; C: species concentration; C_p: specific heat at constant pressure; C_s: concentration susceptibility; D_m: mass diffusivity; Du: Dufour number; Ec: Eckert number; g: acceleration due to gravity; $H = (H_{\bar{x}},\ H_{\bar{y}}, 0)$ induced magnetic field at a point $(\bar{x}, \bar{y}, \bar{z})$; H_x: non-dimensional induced magnetic field intensity; H_0: strength of imposed transverse magnetic field; K_T: thermal diffusion ratio; M: Hartmann number; N: radiation parameter; Nu: Nusselt number; P: non-dimensional pressure gradient; $\bar{P}$: dimensional pressure gradient; Pr: Prandtl number; Re: Reynolds number; Rm: magnetic Prandtl number; Sc: Schmidt number; Sh: Sherwood number; Sr: Soret number; T: temperature; $\bar{u}$: fluid velocity component along $\bar{x}$ axis; u: non-dimensional fluid velocity component along x axis; $\bar{v}$: fluid velocity along $\bar{y}$ axis; V: suction/injection velocity; (x, y, z): non-dimensional Cartesian coordinates; $(\bar{x}, \bar{y}, \bar{z})$: dimensional Cartesian coordinates; $\bar{\alpha}$: is the mean absorption coefficient; ϕ: non-dimensional concentration; η: magnetic diffusivity.

REFERENCES

Adesanya, S.O. and Makinde, O.D. (2014) MHD oscillatory slip flow and heat transfer in a channel filled with porous media. *U.P.B. Sci. Bull., Series A*. **76**, 197-204.

Ahmed, N. (2019) Heat and mass transfer in MHD Poiseuille flow with porous walls. *Journal of Engineering Physics and Thermophysics*. **92**, 122-131.

Alam, M.S. and Rahman, M.M. (2006) Dufour and Soret effects on mixed convection flow past a vertical porous flat plate with variable suction. *Nonlinear Anal: Model control*. **11**, 3-12.

Beavers, G.S. and Joseph, D.D. (1967) Boundary conditions at a naturally permeable wall. *Journal of Fluid Mechanics*. **30**, 197-207.

Bilal, A.M., Hayat, T. and Alhuthali, M.S. (2015) Three dimensional flow of Maxwell fluid with Soret and Dufour effects. *J Aerosp Eng.* **29**, 04015065.

Brewster, M. Q. (1992) *Thermal Radiative Transfer and Properties*, John Wiley & Sons, New York.

Choudhury, R. and Das, U.J. (2012) Heat Transfer to MHD Oscillatory Viscoelastic Flow in a Channel Filled with PorousMedium. *Physics Research International.* Article ID 879537.

Cox, S.M. (1991) Two dimensional flow of a viscous fluid in a channel with porous walls. *J Fluid Mech.* **227**, 1-33.

Das, U. J. (2017) Heat transfer to MHD oscillatory dusty visco-elastic fluid flow in an inclined channel filled with a porous medium. *Latin American Applied Research*. **47**, 145-150.

Divya, B.B., Manjunatha, G., Rajashekhara, C., Vaidyab, Hanumesh and Prasad, K.V. (2019) Impact of variable liquid properties on peristaltic mechanism of convectively heated Jeffrey fluid in a slippery elastic tube. *Frontiers in Heat and Mass Transfer*. **12** (2019).

Hayat, T., Zahir, H., Tanveer, A. and Alsaedi, A . (2018) Soret and Dufour effects on MHD peristaltic flow of Prandtl fluid in a rotating channel. *Results in Physics*. **8**, 1291-1300.

Khaled, A.R.A and Vafai, K. (2004) The effect of the slip condition on Stokes and Couette flows due to an oscillating wall: exact solutions. *Int. J. Non-linear Mech.* **39**, 795-809.

Makinde, O.D (2011) On MHD mixed convection with Soret and Dufour effects past a vertical plate embedded in a porous medium. *Latin American Applied Research*. **41**, 63-68.

Makinde, O.D. and Osalusi, E. (2006) MHD steady flow in a channel with slip at the permeable boundaries. *Rom. J. Phys.* **51**, 319-328.

Makinde, O.D. and Mhone, P.Y. (2005) Heat transfer to MHD oscillatory flow in a channel filled with porous medium. *Rom J Phys*. **50**, 931-938.

Manjunatha, G., Rajashekhar, C., Vaidya, Hanumesh, Prasad, K. V., Makinde, O. D. and Viharika, J. U. (2020) Impact of Variable Transport Properties and Slip Effects on MHD Jeffrey Fluid Flow Through Channel. *Arabian Journal for Science and Engineering*. **45**, 417-428.

Manjunatha, G., Vaidya, H., Rajashekhar, C. and Prasad, K.V. (2019) Peristaltic flow of a Jeffery fluid with heat transfer in an inclined porous tube under the influence of slip and variable viscosity. *Defect and Diffusion Forum*, 16-30.

Mehmood, A. and Ali, A. (2007) The effect of slip condition on unsteady MHD oscillatory flow of a viscous fluid in a planner channel. *Rom. J. Phys.* **52**, 85-91.

Misra, J.C. Adhikary, S.D. (2016) MHD oscillatory channel flow, heat and mass transfer in a physiological fluid in presence of chemical reaction. *Alexandria Engineering Journal.* **55**, 287-297.

Soltani, F. and Yilmazer, U. (1998) Slip velocity and slip layer thickness in flow of concentrated suspensions, *J. appl. Polym. Sci*. **70**, 515-522.

Soundalgekar, V.M. and Bhat, J.P. (1984) Oscillatory MHD channel flow and heat transfer. *Indian J Pure Applied Math*. **15**, 819-828.

Srinivas, S., Kumar, C.K. and Reddy, A.S. (2018) Pulsating flow of Casson fuid in a porous channel with thermal radiation, chemical reaction and applied magnetic field. *Nonlinear Analysis: Modelling and Control*. **23**, 213-233.

Turkyilmazoglu, M. and Pop, I. (2012) Soret and heat source effects on the unsteady radiative MHD free convective flow from an impulsively started infinite vertical plate. *Int J Heat Mass Transfer*, **55**, 7635-7644.

Received: July 24, 2020
Sent to Subject Editor: January 13, 2021
Accepted: April 4, 2021
Recommended by Subject Editor Gianfranco Caruso